Mem. S.A.It. Vol. 85, 417

Memorie della

The mass-metallicity relation of galaxies up to redshift 0.35

I. Saviane[1], I. Yegorova[1], D. Proust[2], F. Bresolin[3], V. Ivanov[1], E. V. Held[4], J. Salzer[5], and R. M. Rich[6]

[1] European Southern Observatory, Alonso de Cordova 3107, Santiago, Chile
e-mail: isaviane@eso.org
[2] Observatoire de Paris-Meudon, GEPI, F92195 MEUDON, France
[3] Institute for Astronomy, 2680 Woodlawn Drive, Honolulu, HI 96822, USA
[4] Astronomical Observatory, vicolo Osservatorio 5, Padova, Italy
[5] Department of Astronomy, Indiana University, 727 East Third Street, Bloomington, IN 47405, USA
[6] Division of Astronomy & Astrophysics, University of California, 430 Portola Plaza, Los Angeles, CA 90095-1547, USA

Abstract. Our research on the age-metallicity and mass-metallicity relations of galaxies is presented and compared to the most popular investigations in the field. We have been able to measure oxygen abundances using the direct method for objects spanning four orders of magnitude in mass, and probing the last 4 Gyr of galaxy evolution. We have found preliminary evidence that the metallicity evolution is consistent with expectations based on age-metallicity relations obtained with low resolution stellar spectra of resolved Local Group galaxies.

Key words. Galaxies: abundances – Galaxies: evolution – Galaxies: fundamental parameters – Galaxies: ISM – Galaxies: star formation

1. Introduction

Forty years ago Larson (1974) attempted one of the first theoretical investigations to explain the mass-metallicity relation (MZR) of (elliptical) galaxies. His final relation is remarkably similar to current observational results: the metallicity goes from [m/H]~ -2.3 at $M = 10^5 M_\odot$ to [m/H]$\sim$ 0 at $M = 10^{13} M_\odot$, and it flattens at high masses. To test these kind of predictions we can either reconstruct the age-metallicity relation (AMR) of galaxies of different masses, or go back in time by taking snapshots of the MZR at different redshifts.

2. Age-metallicity relations of resolved galaxies

Thanks to the advent of moderate resolution, multiplexing spectrographs at 10m-class telescopes, AMRs are now available for several resolved galaxies in the Local Group. As an example, in Gullieuszik et al. (2009) we measured the metallicity of 54 red-giant stars in the dSph galaxy Leo I by applying the CaT method (Armandroff & Da Costa 1991), and we found individual ages by interpolating a set of isochrones. Similar methods are employed by other groups: for example Leaman et al.

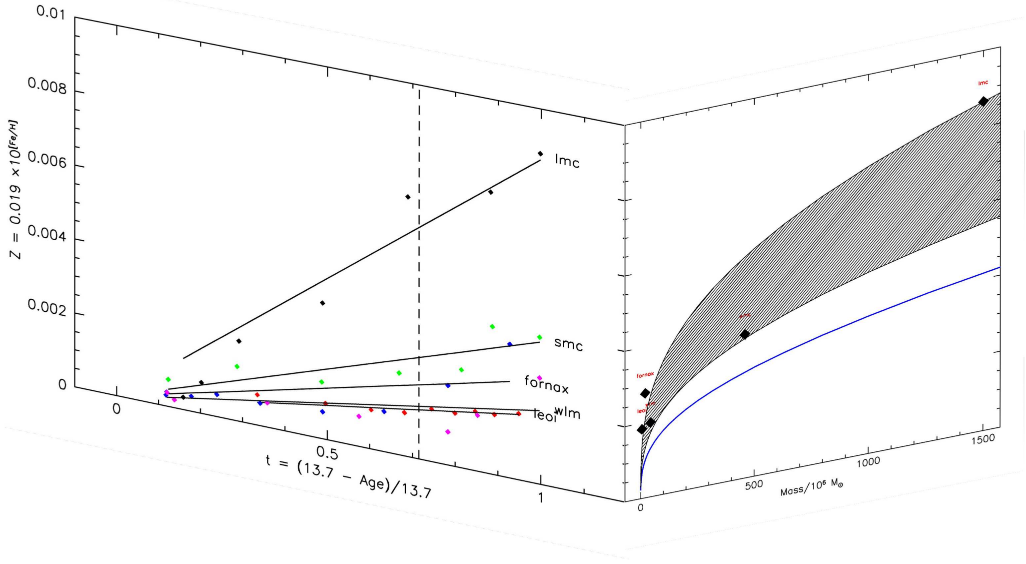

Fig. 1. The left side of the box shows age-metallicity relations from Leaman et al. (2013) and Gullieuszik et al. (2009). The vertical dotted line marks redshift $z = 0.35$. The right side shows the terminal points of the linear AMRs against present galaxy mass (with mass from McConnachie 2012). The blue curve is the mass-metallicity relation from Kirby et al. (2011), which represents the evolutionary status of galaxies some time in the past. The shaded area shows the effect of evolution assuming that current metallicities are a factor 1.6 higher than those of K11 (the area encompasses the $\pm 1\sigma$ error from K11).

(2013) published AMRs for Fornax, WLM, and the Magellanic clouds. These relations can be seen in Fig. 1 together with that of Leo I. The figure shows that a linear growth of Z vs. time is a reasonable approximation, and in addition, if the end points of the AMRs are plotted vs. mass, then there is a good correlation between mass and metallicity. Therefore as long as stellar mass grows with time, one can expect a well defined MZR at any age (redshift), at least as far as dwarf galaxies are concerned. In particular at redshift $z = 0.35$ the universe is $\sim 70\%$ its current age so we can expect a factor 1.4 increase in Z since that time, or 0.14 dex in [m/H].

3. Snapshots of the MZR at different redshifts

Exploring the MZR at different redshifts is an active research field where we are carrying out our own investigation since a few years. Some of the major recent studies can be found in, e.g, Tremonti et al. (2004), Pettini & Pagel (2004), Erb et al. (2006), Kobulnicky & Kewley (2004), Savaglio et al. (2005), Lee et al. (2006), Maiolino et al. (2008), Zahid et al. (2013).

3.1. Local universe

Our relation for dIrr galaxies in nearby groups has been published in Saviane et al. (2008) (hereafter, S08), and we are currently working on data for galaxies in the local universe, and for members of the AC 114 cluster at redshift 0.35. The aim is to extend the MZR from dwarf to massive galaxies, and to observe its evolution with redshift. The main feature of our investigation is that we are trying to use the direct method for the whole mass range, which is quite demanding in terms of observing time because it requires to measure faint auroral lines. This task becomes es-

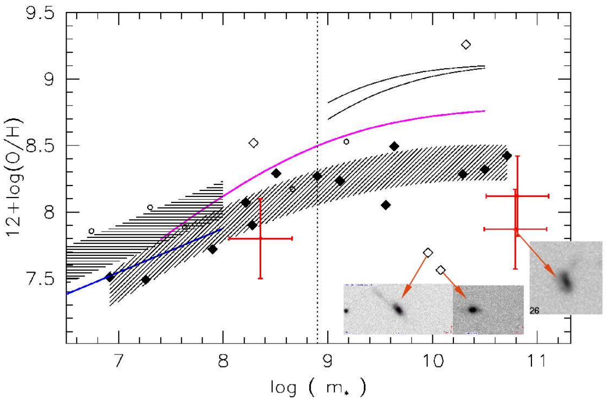

Fig. 2. Several MZR are represented in this figure: the open and filled diamonds are data from Saviane et al. (2008) (to the left of the vertical dotted line) and from papers in preparation. The blue curve and horizontally hashed area are the MZR from Kirby et al. (2011) and the same MZR with an offset by 0.22 dex (like in Fig. 1); the other hashed area is the MZR from Saviane et al. (in preparation). Open small circles are present-day metallicities reached by the AMRs of Fig. 1. The magenta curve is the MZR from Andrews & Martini (2013), and the two short curves are MZRs from Zahid et al. (2013) for $z = 0.08$ and $z = 0.29$ (upper and lower curve, respectively). Finally red diamonds with error bars are the three star-forming galaxies in AC114 where we could compute abundances via the direct method. The inset images show that AC114 and KISS galaxies with abundances that are more than 3σ lower than the average, show signs of being accreting fresh gas.

pecially difficult for massive galaxies, which are usually more metal-rich than dwarfs: when metals become more abundant, gas cooling by atomic lines becomes more effective, and the dropping temperature reduces emissivities. Therefore the so-called empirical method is much more popular, because it uses strong nebular lines that are much easier to measure. Very large galaxy samples can thus be easily built. An interesting exception to this trend is the recent study of Andrews & Martini (2013, hereafter AM13), where SDSS spectra were stacked to boost the signal-to-noise ratio of [O III]λ4363. In this way, the electron temperature could be calculated even for galaxies at the top end of the mass function, using the line ratio [O III]λ4363/[O III]$\lambda\lambda$4959,5007. To extend our study to massive galaxies, we obtained Keck/LRIS spectra of objects from the KISS survey (Salzer et al. 2000). We have been able to measure central oxygen abundances for eleven targets, using either the quoted oxygen line ratio, or [N II]λ5755/[N II]$\lambda\lambda$6548,6583. Fig. 2 shows that these objects extend the S08 MZR to larger masses. There are also two low-metallicity objects, which might be accreting fresh gas that could be diluting their abundances: indeed broad-band imaging shows clear signs of filaments departing from the central bodies. Another feature of our project is the usage of H-band imaging to compute target luminosities: because the SEDs of low-mass stars peak near that band, H-band luminosities are much less sensitive to individual star-formation histories, when compared to optical luminosities (Bell & de Jong 2001). Figure 2 shows two other MZRs for the local universe, from AM13 and Zahid et al. (2013, hereafter Z13). The relation from Z13 is fairly representative of MZRs obtained with the empirical method, and it is well above our own. To a lesser extent this is true for the AM13 relation as well. An independent metallicity constraint for massive galaxies can be given by stellar abundances for young stars in our own Milky Way. For example based on Cepheid data Luck et al. (2011) find a well-defined metallicity gradient reaching ~

0.3 dex above solar at their minimum radius of ∼ 4 kpc. Extrapolating their linear relation of -0.055 dex kpc^{-1} one might expect [Fe/H]=0.5 dex in the center. When measuring unresolved galaxies, the observed metallicity will be averaged within the aperture of the spectrograph: taking into account this effect, the effective gradient becomes shallower, such that within an aperture encompassing 16 kpc of radius a metallicity [Fe/H]=0.1 dex would be observed. Therefore, as long as the MW represents typical massive disk galaxies, we can expect oxygen abundances varying between 12 + log(O/H) ∼ 8.8 and ∼ 9.2 depending on the disk fraction that falls into the spectrograph aperture. This range is almost the same that is comprised between the MZRs of AM13 and Z13 at $\log M_* = 10.5$, so based on this exercise we would also expect the "true" MZR to fall between those two relations (both based on SDSS7 data). Uncertainties of the empirical method have been discussed, e.g., in Kewley & Ellison (2008), but it is also possible that the direct method underestimates abundances (Nicholls et al. 2013). Because our MZR stays below that of AM13 and both are based on the direct method, it is possible that our targets are intrinsically different than the average object of the SDSS: for example a 0.2 dex lower metallicity could be the attribute of objects with SFR ∼ 100 times larger than the SDSS average (Mannucci et al. 2010). The fact that different classes of galaxies follow different MZRs is supported by noting in Fig. 2 how dIrr galaxies stay below the end points of the AMRs of dSph/dE galaxies. dIrr galaxies evolve more slowly than dSph/dE because of their low SFRs (e.g., Momany et al. 2005).

3.2. Emission line galaxies in AC114

Studies of the MZR are now available up to $z =$ 3.5 Laskar et al. (2011), but one possible problem when comparing relations at different redshifts, is that metallicities can be obtained with different calibrations of the empirical method, thus rendering both absolute values and relative trends uncertain. In addition, it is not clear whether calibrations based on local H II regions should be valid at high redshift, where the physical conditions of the ISM might be different. To bypass this problem we are trying to obtain direct metallicities of emission-line galaxies in cluster AC114 at $z = 0.35$. At this redshift all important emission lines still fall in the optical range, so though 0.35 sounds modest compared to other works, abundances can be obtained with higher precision thus potentially revealing even a small evolution. The 0.14 dex predicted in Sec. 2 should certainly be within reach. Optical spectra of 153 galaxies in the field of AC114 were obtained with 5h exposures in each of the HR red and MR grisms of VIMOS at the VLT. With a kinematic analysis of recession velocities (Proust et al., in preparation) we could select 21 emission-line galaxies over a total of 86 cluster members, and for three of them [O III]λ4363 could be detected. We are in the process of refining the extraction to arrive at detection in more objects. The red crosses in Fig. 2 show the location of the three galaxies in the MZ plane. At $z = 0.35$ rest-frame H-band moves into K-band, but unfortunately there is no comprehensive NIR photometric catalog for AC114. The brightest two galaxies have R-band COSMOS photometry (Capak et al. 2007; Tasca et al. 2009), which corresponds to V-band in rest-frame. This means that luminosities can be affected by recent star-formation, so our masses computed with a fiducial $M/L = 2$ could be underestimated. Therefore we attributed error bars of a factor of two to the masses of these galaxies. Absolute luminosities were calculated assuming a luminosity distance of 1540 Mpc. Interestingly, one of the two luminous objects has lower abundance than the other, but it seems to be accreting material, so it might be another case of fresh gas diluting the ISM abundance (see Fig. 2). If the other galaxy can be considered a typical undisturbed cluster member, then it has an oxygen abundance ∼ 0.2 dex lower than our local MZR, roughly in agreement with the predictions of Sec. 2. There is no COSMOS photometry for the third galaxy, so we just assigned it a value $R = 25$, which is the faintest value of the catalog.

4. Conclusion

Thanks to our original dataset, and the homogeneous method of analysis, we have been able to detect an evolution with redshift of the MZR for the massive galaxies in our samples. If their AMRs were linear with time, then the evolution would be consistent with the 0.14 dex expected from reconstructed relations for less massive galaxies over the last 4 Gyr. Considering all possible scenarios, the true MZR for normal disk galaxies is probably close to that of AM13. Fig. 1 shows that the MZR is a direct consequence of the rate of metal production dZ/dt increasing with mass. In a closed-box scenario coupled with the Schmidt (1959) law, this would not be surprising. The model predicts that the metal production rate is $dZ/dt = -p/M_{\rm gas}\, dM_{\rm gas}/dt = -p/M_{\rm gas}\,$SFR, where p is the metal yield and $\mu = M_{\rm gas}/M_{\rm TOT}$ is the mass fraction of gas (Searle & Sargent 1972); and the Schmidt law tells us that SFR is proportional to gas density. Given that gas density is proportional to $M\,R^{-3}$, and that mass varies much more than size among galaxies, it is expected that metal production ultimately depends on galaxy mass. Of course gas exchanges with the environment will happen during the life of a galaxy, so metallicity can drop below, or can be driven above that predicted in this simple scenario. Still, Fig. 2 seems to suggest that other processes play a secondary role in the definition of the AMR. Note also that Rodrigues et al. (this volume) find that intermediate mass galaxies evolved as closed systems in the past 6 Gyr. If Z increases linearly with time, then setting dZ/dt = const gives both $M_{\rm gas}$ and SFR=$dM_{\rm gas}/dt \propto e^{-kt}$. An exponential decay in time of the SFR could then be the symptom of a system with little gas exchanges with the environment.

References

Andrews, B. H. & Martini, P. 2013, ApJ, 765, 140
Armandroff, T. E. & Da Costa, G. S. 1991, AJ, 101, 1329
Bell, E. F. & de Jong, R. S. 2001, ApJ, 550, 212
Capak, P., Aussel, H., Ajiki, M., et al. 2007, ApJS, 172, 99
Erb, D. K., Shapley, A. E., Pettini, M., et al. 2006, ApJ, 644, 813
Gullieuszik, M., et al. 2009, A&A, 500, 735
Kewley, L. J. & Ellison, S. L. 2008, ApJ, 681, 1183
Kirby, E. N., et al. 2011, ApJ, 727, 78
Kobulnicky, H. A. & Kewley, L. J. 2004, ApJ, 617, 240
Larson, R. B. 1974, MNRAS, 169, 229
Laskar, T., Berger, E., & Chary, R.-R. 2011, ApJ, 739, 1
Leaman, R., Venn, K. A., Brooks, A. M., et al. 2013, ApJ, 767, 131
Lee, H., Skillman, E. D., Cannon, J. M., et al. 2006, ApJ, 647, 970
Luck, R. E., et al. 2011, AJ, 142, 51
Maiolino, R., Nagao, T., Grazian, A., et al. 2008, A&A, 488, 463
Mannucci, F., et al. 2010, MNRAS, 408, 2115
McConnachie, A. W. 2012, AJ, 144, 4
Momany, Y., Held, E. V., Saviane, I., et al. 2005, A&A, 439, 111
Nicholls, D. C., Dopita, M. A., Sutherland, R. S., Kewley, L. J., & Palay, E. 2013, ApJS, 207, 21
Pettini, M. & Pagel, B. E. J. 2004, MNRAS, 348, L59
Salzer, J. J., Gronwall, C., Lipovetsky, V. A., et al. 2000, AJ, 120, 80
Savaglio, S., Glazebrook, K., Le Borgne, D., et al. 2005, ApJ, 635, 260
Saviane, I., Ivanov, V. D., Held, E. V., et al. 2008, A&A, 487, 901
Schmidt, M. 1959, ApJ, 129, 243
Searle, L. & Sargent, W. L. W. 1972, ApJ, 173, 25
Tasca, L. A. M., Kneib, J.-P., Iovino, A., et al. 2009, A&A, 503, 379
Tremonti, C. A., Heckman, T. M., Kauffmann, G., et al. 2004, ApJ, 613, 898
Zahid, H. J., Geller, M. J., Kewley, L. J., et al. 2013, ApJ, 771, L19